Journal of Medical Ultrasonics (2019) 46:81–88
https://doi.org/10.1007/s10396-018-0886-x

ORIGINAL ARTICLE

Correlation between acoustic radiation force impulse (ARFI)-based tissue elasticity measurements and perfusion parameters acquired by perfusion CT in cirrhotic livers: a proof of principle

Michael Esser[1] · Michael Bitzer[2] · Manuel Kolb[1] · Jan Fritz[3] · Mustafa Kurucay[1] · Christer Ruff[1] · Marius Horger[1]

Received: 9 March 2018 / Accepted: 21 May 2018 / Published online: 13 June 2018

Abstract

Purpose To investigate whether liver stiffness measured by acoustic radiation force impulse (ARFI) sonoelastography always correlates with the liver perfusion parameters quantified by perfusion CT in patients with known liver cirrhosis.

Methods Sonoelastography and perfusion CT were performed in 50 patients (mean age 65.5; range 45–87 years) with liver cirrhosis, who were classified according to Child–Pugh into class A (30/50, 60%), B (17/50, 34%), and C (3/50, 6%). For standardized ARFI measurements in the left liver lobe at a depth of 4 cm, a convex 6-MHz probe was used. CT examinations were performed using 80 kV, 100 mAs, and 50 ml of iodinated contrast agent injected at 5 ml/s. Using standardized region-of-interest measurements, we quantified arterial, portal venous, and total liver perfusion.

Results There was a significant linear correlation between tissue stiffness and arterial liver perfusion ($p=0.015$), and also when limiting the analysis to patients with histology ($p=0.019$). In addition, there was a positive correlation between the total blood supply (arterial + portal-venous liver perfusion) to the liver and tissue stiffness ($p=0.001$; with histology, $p=0.027$). Shear wave velocity increased with higher Child–Pugh stages ($p=0.013$).

Conclusion The degree of tissue stiffness in cirrhotic livers correlates expectedly—even if only moderately—with the magnitude of arterial liver perfusion and total liver perfusion. As such, liver elastography remains the leading imaging tool in assessing liver fibrosis.

Keywords Liver cirrhosis · Elasticity imaging techniques · Perfusion imaging · Spiral computed tomography

Introduction

Many chronic liver diseases lead to parenchymal scarring (fibrosis) that replaces healthy liver parenchyma, leading ultimately to liver cirrhosis. In later stages, the altered parenchymal architecture leads to increased vascular flow resistance and increased intravascular pressures in the portal-venous system, and to a lesser degree in the hepatic artery [1]. The increased arterial perfusion compensates for the loss of portal-venous blood supply, which is referred to as hepatic arterial buffer response (HABR) [2]. Hence, portal hypertension and the shift of the dual blood supply of the liver toward hepatic

✉ Michael Esser
michael.esser@med.uni-tuebingen.de

Michael Bitzer
michael.bitzer@med.uni-tuebingen.de

Manuel Kolb
manuel.kolb@med.uni-tuebingen.de

Jan Fritz
jfritz9@jhmi.edu

Mustafa Kurucay
mustafa.kurucay@med.uni-tuebingen.de

Christer Ruff
christer.ruff@med.uni-tuebingen.de

Marius Horger
marius.horger@med.uni-tuebingen.de

[1] Department of Diagnostic and Interventional Radiology, Eberhard-Karls-University, Hoppe-Seyler-Str. 3, 72076 Tübingen, Germany

[2] Department of Internal Medicine I, Eberhard-Karls-University, Otfried-Müller-Str. 10, 72076 Tübingen, Germany

[3] Russell H. Morgan Department of Radiology and Radiological Science, Johns Hopkins University School of Medicine, 601 N. Caroline Street, JHOC 3140A, Baltimore, MD 21287, USA

arterial supply could be used for non-invasive evaluation of the degree of liver parenchymal alteration and consecutive portal hypertension.

A commonly used method for the detection of circulatory alterations of the dual liver blood supply is the measurement of blood flow velocity in the portal vein using Doppler ultrasound [3]. Another more sophisticated method is perfusion CT, which enables separate calculation of the portal venous and hepatic arterial blood contribution to the total liver blood supply. As many patients with liver disease undergo multiphase CT for hepatocellular carcinoma surveillance and detection of complications, this information could additionally be obtained as a surrogate marker for parenchymal alterations.

The diagnosis of cirrhosis is usually suggested by history, physical examination, and blood tests, but confirmation is sometimes still needed and requires liver biopsy as a gold standard for diagnosis of liver fibrosis. Tissue sampling is invasive, prone to complications, and can fail to diagnose cirrhosis, because the tissue samples may not be representative for the entire liver [4].

Sonoelastography measures the tissue elasticity of liver parenchyma and has emerged as a reliable tool to diagnose liver cirrhosis [5]. Increased stiffness of liver parenchyma, which occurs in chronic liver diseases, results in faster propagation of mechanical waves, which allows for the differentiation of normal liver parenchyma from liver fibrosis and cirrhosis [6]. Among the different sonoelastography techniques, acoustic radiation force impulse (ARFI) is commonly used as it is independent of the investigator and, thus, more accurate [6–9].

Although the approaches of perfusion CT and sonoelastography for diagnosing liver fibrosis and cirrhosis are totally different, we hypothesized that they might correlate, given that microvascular damage leading to increased resistance of vascular flow occurs together with parenchymal scarring, fibrosis, and cirrhosis. In this context, we assume that multimodality imaging may provide useful tissue information to potentially reduce the number of required liver biopsies and to avoid possible associated complications, as mentioned above.

Therefore, the aim of our study was to quantify changes in the pathophysiological pathways of liver cirrhosis, and to correlate sonoelastography parameters that are suggestive of hepatic fibrosis with those of perfusion CT and the clinical Child–Pugh stage.

Materials and methods

Study design

The study was approved by the institutional review board. Fifty patients (46 males and 4 females; mean age 65.5 years, range 45–87 years) with liver cirrhosis were enrolled consecutively between August and December 2016. All patients underwent whole-liver perfusion CT and ultrasound elastography on the same day. Image data analyzed in this study were acquired prospectively as part of a routine examinational work-up at our institution meant to detect hepatocellular carcinoma in cirrhotic livers. Informed consent was obtained from all individual participants included in the study. For data evaluation and comparison of the two imaging modalities, retrospective approval was requested from our institutional review board with a waiver of informed consent. All procedures performed in studies involving human participants were in accordance with the ethical standards of the institutional committee and with the 1964 Helsinki declaration and its later amendments or comparable ethical standards.

Inclusion criterion was the presence of liver cirrhosis. As a standard of reference, hepatic cirrhosis was proven by histology (biopsy) in 30/50 (60%) subjects, whereas, in 20/50 (40%) subjects, liver cirrhosis was diagnosed by the combination of abnormal liver function tests and imaging characteristics such as signs of liver cirrhosis on gray-scale ultrasound.

In addition, 25/50 (50%) subjects had a history of alcohol abuse, 14/50 (28%) viral infection, 7/50 (14%) no contributing history, 2/50 (4%) hemochromatosis, and 2/50 (4%) non-alcoholic fatty liver disease. Hepatocellular carcinoma was found in 35/50 (70%) subjects. Diagnosis of hepatocellular carcinoma was made by histology (26/35, 74%) or according to the current diagnostic guidelines in patients with hepatocellular carcinoma based on typical contrast-enhancement patterns (9/35, 26%) [3]. Larger HCCs or those located close to the left liver lobe including those with macrovessel invasion were excluded from the final evaluation.

Patients were excluded from the study when solely invalid shear wave values were detected or when perfusion CT analysis could not be realized. Three patients were excluded from the analysis because of portal vein thrombosis ($n=2$) and inadequate contrast in the portal venous contrast agent phase ($n=1$). Accordingly, 47 patients remained for the final analysis.

All patients were classified according to Child–Pugh score based on the serum concentrations of bilirubin and albumin, the international normalized ratio (INR), the presence or absence of ascites, and the degree of encephalopathy into stages A, B, or C [10, 11].

Sonoelastography technique

Acoustic radiation force impulse liver elastography was performed with the Acuson S3000 (Siemens Medical Solutions, Mountain View, CA, USA) using a curved-array probe (6C1, Siemens) with a bandwidth of 1.5–6 MHz by two staff

radiologists, each with 2 years of experience in sonoelastography. This device generates shear waves by means of short push pulses (mean 2.67 MHz).

The left liver lobe was used to place standardized regions of interest (ROI), due to its good accessibility to elastography measurements as it lies directly behind the body wall near the probe.

ARFI measurements were used to measure shear wave velocities (SWV) in the liver parenchyma (Fig. 1a). A 10 × 6-mm ROI was placed under ultrasound control, avoiding identifiable blood vessels and biliary structures at a mean depth of 4 cm (range 3–6 cm) from the skin to standardize quantification. As Virtual Touch™ tissue quantification expresses the SWV in solid materials as numerical values, only numerical results (m/s) were used for this study. A minimum of three measurements was taken in each patient. Non-valid measurements due to erroneous ROI positioning (i.e., vessels or biliary structures within the ROI or patient motion) were excluded. Patients were examined in a supine position using the breath-hold technique. All examinations were performed using a subcostal position. Minimal scanning pressure was applied by the operator. Patients were advised to fast before ultrasound elastography (USE).

Perfusion CT technique

CT examinations were part of standard imaging surveillance of hepatocellular carcinoma in patients with liver cirrhosis at our institution and were always indicated by the treating physicians, independent of the current study. All CT examinations were performed on a 256-slice MDCT scanner (SOMATOM Definition Flash; Siemens Healthcare, Forchheim, Germany). Perfusion CT covered the entire liver in the *z*-axis at 80-kVp, 100-mAs, 64 × 0.6-mm collimation, scan time of 40 s, and time resolution of 1.5 s per acquired spiral data set [7, 8, 12]. Following a start delay of 7 s, a total of 50-ml Ultravist 370 (Bayer Vital, Leverkusen, Germany) was injected intravenously at a flow rate of 5 ml/s and followed by 50-ml saline flush. One set of axial images with a slice thickness of 3 mm for perfusion analysis was reconstructed with a medium smooth tissue convolution kernel (B10f) and transferred to an external workstation (Multi-Modality Workplace, Siemens Healthcare) for analysis.

Perfusion CT analysis

Perfusion CT data were analyzed using Syngo Volume Perfusion CT Body (Siemens Healthcare). The algorithms are based on non-rigid deformable registration for anatomic alignment and a dedicated noise reduction technique for dynamic data [13, 14].

Perfusion parameter maps of arterial liver perfusion (ALP; ml/100 ml/min), portal-venous perfusion (PVP; ml/100 ml/min), and hepatic perfusion index (HPI; %) were determined for the assessment of dual liver parenchymal blood supply using the maximum-slope calculation technique (Fig. 1b) [8]. Determination of ALP and PVP—according to the dual blood supply of the liver by the hepatic artery and portal vein—was done using the time of peak splenic enhancement by drawing ROIs in the portal vein and spleen, respectively. Arterial time density curve for ALP was calculated by dividing the maximum arterial slope by maximum aortic enhancement. Portal-venous time density curve for PVP was calculated by dividing the maximum portal-venous slope by maximum portal vein enhancement. HPI in % represents ALP divided by the sum of ALP and PVP [8]. The total liver perfusion (TLP) was calculated by adding ALP to PVP.

Statistical analysis

For statistical analysis, IBM SPSS Statistics (Ver. 22 for Windows, Ehningen, Germany) was used. Using univariate analysis of variance, the influence of Child–Pugh stage, ultrasound probe, and presence of hepatocellular carcinoma on SWV was identified, taking also sex and age as covariates into consideration. The normality Shapiro–Wilk test was applied to study the distribution of quantification data. Spearman's rank correlation coefficient with two-tailed *t* test was used to analyze the relationship between SWV and perfusion CT parameters. A *p* value less than 0.05 was considered to indicate statistical significance.

Results

Ultrasound elastography and perfusion CT parameters

The median SWV was 2.7 m/s [range 1.3–4.5 m/s, interquartile range (IQR) 2.0–3.6 m/s]. The median values of ALP and PVP were 13.2 ml/100 ml/min (range 2.2–46.1 ml/100 ml/min; IQR 7.1–18 ml/100 ml/min) and 8.4 ml/100 ml/min (range 1.6–34.3 ml/100 ml/min; IQR 6–13.6 ml/100 ml/min), respectively. The resulting TLP showed a median value of 21.8 ml/100 ml/min, ranging from 11.1 to 47.7 ml/100 ml/min (IQR 19.2–26.6 ml/100 ml/min). The median HPI value was 56.2% (range 10.1–96.7%, IQR 37.3–74.1%). There was one outlier with an extremely high HPI value (96.7%).

Shapiro–Wilk test indicated that the perfusion CT parameters did not follow a normal distribution ($p < 0.001$).

There was a significant linear correlation between the SWV and ALP ($p = 0.015$, $r = 0.35$, Fig. 2) and TLP ($p = 0.001$, $r = 0.46$, Fig. 3). There were three outliers in terms of ALP measurements that notably differed. There was

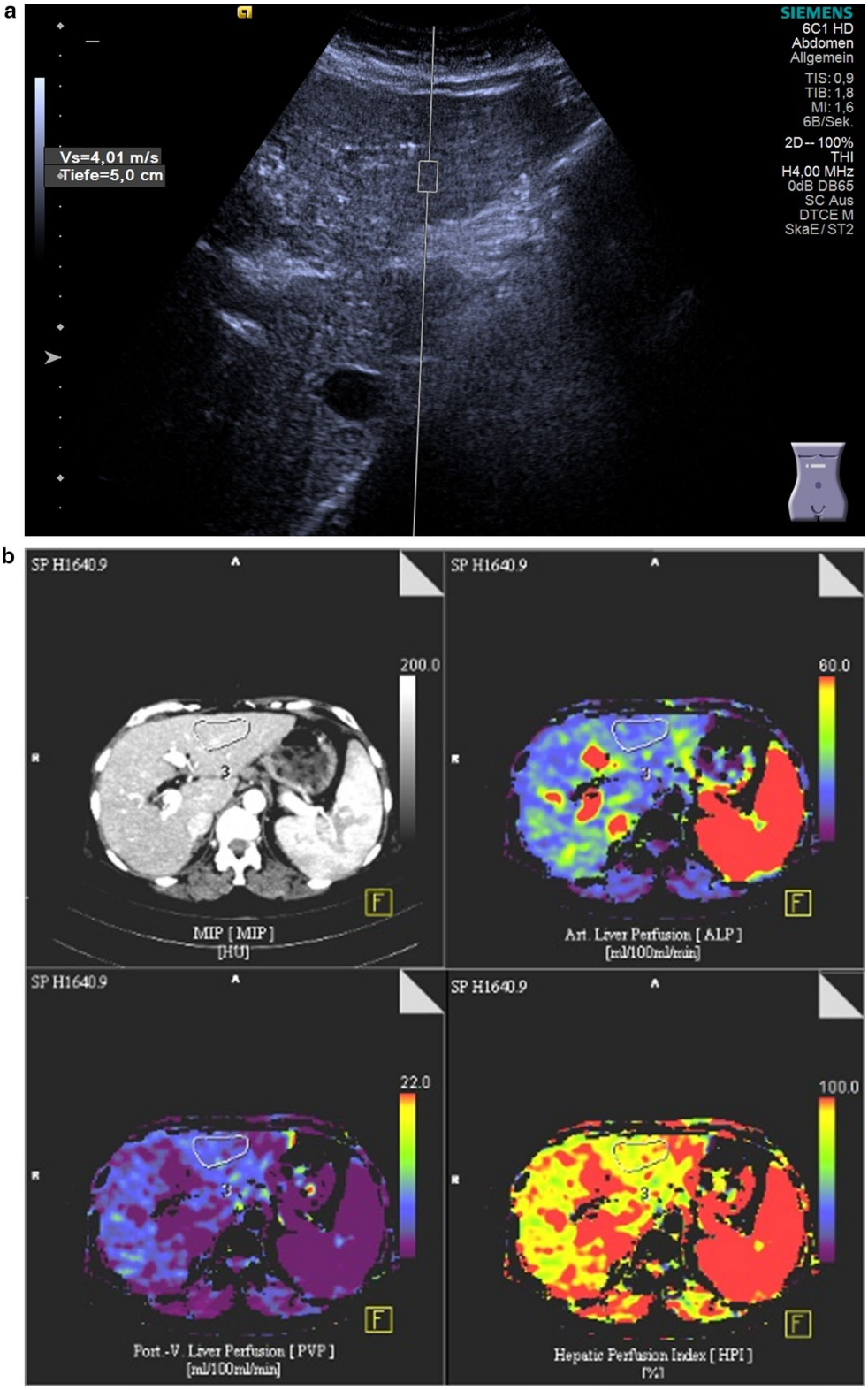

Fig. 1 Acoustic radiation force impulse (ARFI) elastography and perfusion computed tomography. **a** 61-year-old woman with histologically proven cryptogenic liver cirrhosis (Child–Pugh stage A). B-mode US image and corresponding ARFI are presented with a single ROI placed 5 cm below the skin surface. **b** Four perfusion CT color-coded maps of the same patient showing maximum intensity projection (MIP) image, arterial liver perfusion (ALP, 21.3 ml/100 ml), portal-venous perfusion (PVP, 4.7 ml/100 ml), and hepatic perfusion index (HPI, 82.6%) with placement of the ROI in the left liver lobe

no linear correlation between the SWV and PVP ($p = 0.8$, $r = -0.03$) or HPI ($p = 0.13$, $r = 0.22$).

When limiting the analysis to patients with liver cirrhosis diagnosed by needle biopsy and histology ($n = 30$), linear correlations could still be found between SWV and ALP ($p = 0.019$, $r = 0.43$) and TLP ($p = 0.027$, $r = 0.41$). In this subgroup, there was also no linear correlation between

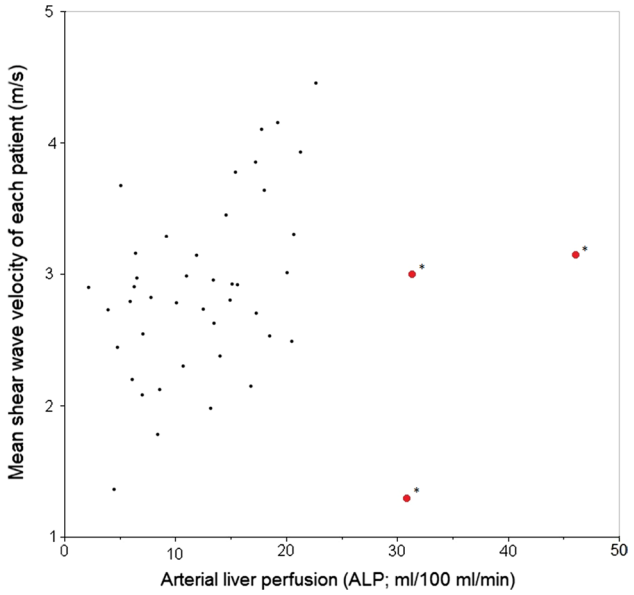

Fig. 2 Mean shear wave velocity (SWV) by arterial liver perfusion (ALP). Dot plot of mean shear wave velocities (SWV; in m/s) of each subject against arterial liver perfusion (ALP; in ml/100 ml/min) values demonstrates a linear correlation between the two parameters ($p=0.015$, $r=0.35$). Three outliers are highlighted in red (asterisks)

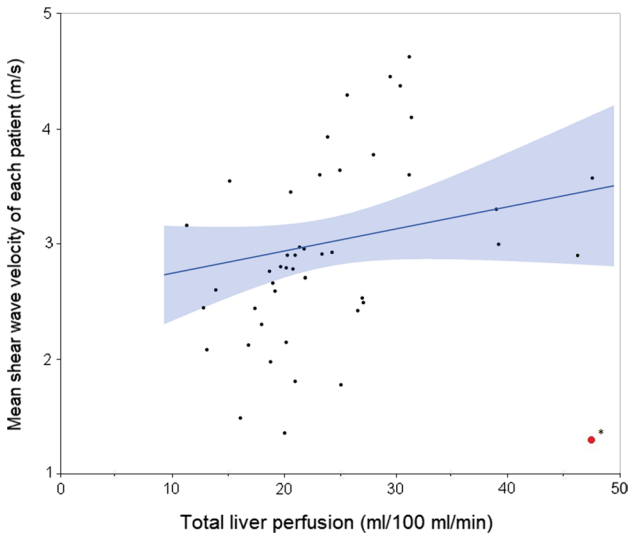

Fig. 3 Mean shear wave velocity (SWV) by total liver perfusion (TLP). Dot plot of mean shear wave velocities (SWV; in m/s) of each subject against total liver perfusion (TLP; in ml/100 ml/min) values demonstrates a linear correlation between the two parameters ($p=0.001$, $r=0.46$). One outlier is highlighted in red (asterisk). In addition, linear regression analysis was performed and regression bands are shown

the SWV and PVP ($p=0.45$, $r=-0.15$) or HPI ($p=0.12$, $r=0.3$).

When limiting the analysis to patients with a history of alcohol abuse ($n=23$), there was no linear correlation between SWV and the perfusion parameters, but only a slight trend towards a relation between SWV and TLP ($p=0.19$, $r=0.30$).

Child–Pugh scores

Mild hepatic impairment was found in 30/50 (60%) subjects (Child A), while 17/50 (34%) subjects presented with liver cirrhosis Child–Pugh class B, and 3/50 (6%) subjects had severe hepatic dysfunction (Child C).

In liver cirrhosis Child class A, the median SWV was 2.5 m/s (range 1.3–4.4 m/s, IQR 1.8–3.2 m/s), whereas patients classified as Child B showed a median SWV of 2.8 m/s (range 1.3–4.5 m/s, IQR 2.4–3.6 m/s). The Child C group had a median SWV of 3.9 m/s (range 3.8–4.5 m/s, IQR 3.8–4.2 m/s). There was a significant linear correlation between Child–Pugh scores and SWV ($p=0.013$, Fig. 4). This finding remained true when only patients with histologically proven liver cirrhosis were included ($n=30$, $p=0.04$).

The presence of hepatocellular carcinoma did not influence the SWV values in the contralateral lobe of cirrhotic liver parenchyma ($p=0.64$).

Discussion

Our results show a weak-to-moderate correlation between the degree of liver tissue stiffness and the magnitude of arterial and total blood supply in cirrhotic livers. Although these two measures reflect different adaption mechanisms to the

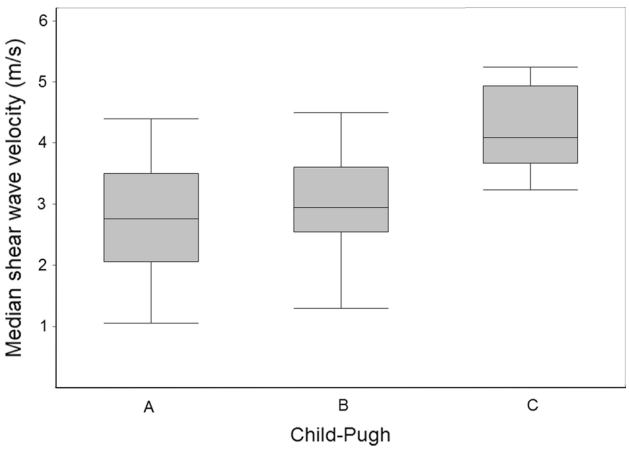

Fig. 4 Shear wave velocity (SWV) by Child–Pugh stage. Box plots showing the median shear wave velocities (SWV; in m/s) with quartile ranges as a function of Child–Pugh subgroups (A–C, $p=0.013$)

continuous damage of liver parenchyma, parallels between these two parameters seem logical, but have not been demonstrated previously to the best of our knowledge.

Increasing fibrosis with consecutive shrinkage of the liver parenchyma leads to stiffer tissue-resisting deformation by the ultrasound push pulses and resulting in a faster propagation of mechanical waves. The change in this mechanical property differentiates normal liver parenchyma from fibrotic liver and cirrhosis. Sonoelastography has advanced to an established diagnostic tool for cirrhosis diagnosis. Using ARFI, the mean SWV measured in our cohort was abnormal in all cases and reached values up to 20 times higher than the normal range. These results are in line with those of earlier reports quantifying tissue elasticity by means of ARFI [15–17]. Changes in the dual liver blood supply in cirrhosis have been analyzed in the past using different imaging techniques [18]. In an animal study, Wang et al. reported the feasibility of perfusion CT in rabbits with the early stages of liver fibrosis and the potential of this technique for assessment of progression of liver fibrosis using PVP, ALP, HPI, BV, and BF [19]. Similar results have been reported by Guan et al. in rats with diffuse liver disease showing continuous changes of liver perfusion parameters with increasing degrees of liver fibrosis up to the stage of liver cirrhosis [20]. Perhaps, the most reliable quantification tool that has been used in the routine diagnosis in the past years for assessment of hepatocellular carcinoma in cirrhotic livers and monitoring response to local or systemic therapy is perfusion CT [21–23]. The feasibility of perfusion CT for blood flow measurements was demonstrated in earlier reports by comparing it with invasive quantification methods like intra-arterially applied microspheres [24]. Its major advantage over dynamic contrast-enhanced MRI studies, for example, is the linear correlation between iodine concentration and tissue attenuation coupled with sophisticated calculation methods that enable separate measurements of arterial and portal-venous blood supply to the liver [25]. Changes in liver parenchymal perfusion occurring in this clinical setting have been described, and they can be subsumed under the term hepatic arterial buffer response (HABR) [2, 18, 25]. Hence, earlier reports demonstrated a decrease in the PVP in favor of the arterial blood supply or a significant change in mean transit time and permeability surface area product measured by perfusion CT in patients with decompensated cirrhosis [18]. Motosugi et al. showed that there was a decrease in PVP in patients with liver cirrhosis [26], whereas van Beers et al. reported that altered hepatic perfusion parameters measured in cirrhosis correlated with the severity of chronic liver disease [27]. However, mechanisms responsible for the HABR are quite complex. They include vasoactive substances like adenosine and nitric oxide, as well as sensory innervation and neuropeptides acting on the microvasculature of the liver to compensate for oxygen deprivation. Moreover, the temporal evolution as well as the magnitude of these adaptive changes may vary considerably [2]. Due to the complexity of these processes and the multitude of mediators, the question to be answered is how far changes in tissue architecture and elasticity are paralleling those of the microvasculature. Experimental data in dogs using perfusion CT have shown significant distinctions between animals with normal livers versus those with fibrotic livers, as well as between fibrosis and cirrhosis in terms of PVP, TLP, and HPI [28]. We found similar results in our study showing significant correlations between Child–Pugh stage and changes in the magnitude of perfusion parameters. Interestingly, not only the ALP but even more the TLP correlated with SWV (Figs. 2, 3). This seems logical and can be considered to represent the influence of the blood volume present in the large capacitance vessels (portal vein, hepatic artery, and hepatic veins) and also the sinusoids [12]. Hence, the compliance of the hepatic vascular bed is expected to correlate with the magnitude of microvascular changes, tissue stiffness, and finally with changes in venous pressure. However, the degree of relationship does not allow for replaceable use of the two techniques for the assessment of increased arterial blood supply to the liver. We would though suggest a complementary use of both approaches for further studies on the subject.

As some of our patients were diagnosed with hepatocellular carcinoma, we additionally looked for the potential impact of an increased arterial supply to the involved liver areas next to the tumors that could have influenced the ALP and TLP values, and subsequently correlated these values with the measured tissue elasticity. Notably, there was no increased arterial supply to the non-involved liver in the vicinity of the tumors, and consecutively no influence on the correlation to liver stiffness. However, in cases with diffuse hepatocellular carcinoma or multifocal ill-defined tumor infiltration, unexpectedly high ALP and HPI values can be measured, as in two of our patients (outliers, Fig. 2), which presumably represents averaging of tumor and liver parenchymal perfusion.

SWV also depends on the depth and the frequency used, with measured values being higher at the same depth for a lower frequency probe [29]. To eliminate the influence of tissue depth on our calculated SWVs, we used a standardized depth for ROI measurements. However, in one overweight patient, we measured SWV at a depth of 6.4 cm, resulting in a disproportionately low value (outlier, Figs. 2, 3).

Our study has limitations. First, the diagnosis of liver cirrhosis was not always proven histologically; hence, investigation of a correlation with the different stages of liver fibrosis and cirrhosis was not possible. However, limitations with biopsy due to heterogeneity in the distribution of cirrhosis are readily known and depend on the site of tissue sampling. Second, the lack of significant correlation between SWV and

PVP might have been caused by the fact that not all patients complied with fasting before the perfusion CT. Knowingly, the portal vein cannot control its blood flow, which is simply the sum of outflows of the extrahepatic splanchnic organs. Third, our SWV and PCT measurements were all performed in the left liver lobe due to the presence of hepatic tumors located in the liver lobe in some of our patients and to the fact that some patients had already undergone right liver surgery (resection) in the past.

Conclusion

Our study confirms that a certain correlation is present between perfusion CT—quantifying arterial and total liver perfusion—and ARFI elastography as a marker for liver tissue alterations in patients with hepatic fibrosis. However, the degree of agreement does not allow for use as a non-invasive tool to evaluate the severity of portal hypertension. Ultrasound and sonoelastography can be regarded as the leading imaging tools in assessing liver fibrosis.

Compliance with ethical standards

Ethical statements All procedures performed in studies involving human participants were in accordance with the ethical standards of the institutional and/or national research committee and with the 1964 Helsinki declaration and its later amendments or comparable ethical standards.

Conflict of interest Michael Esser, Michael Bitzer, Manuel Kolb, Jan Fritz, Mustafa Kurucay, and Christer Ruff declare that they have no conflicts of interest. Marius Horger declares that the institution has received national grants financed by the "Bundesministerium für Bildung und Forschung" (BMBF), Germany.

References

1. Yang YY, Lin HC. Alteration of intrahepatic microcirculation in cirrhotic livers. J Chin Med Assoc. 2015;78:430–7.
2. Eipel C, Abshagen K, Vollmar B. Regulation of hepatic blood flow: the hepatic arterial buffer response revisited. World J Gastroenterol. 2010;16:6046–57 **(Review)**.
3. Bolognesi M, Di Pascoli M, Sacerdoti D. Clinical role of non-invasive assessment of portal hypertension. World J Gastroenterol. 2017;23:1–10.
4. Lee MJ, Kim MJ, Han KH, et al. Age-related changes in liver, kidney, and spleen stiffness in healthy children measured with acoustic radiation force impulse imaging. Eur J Radiol. 2013;82:e290–4.
5. Zhang D, Chen M, Zhou G. The clinical application of acoustic radiation force impulse imaging and transient elastography in chronic hepatitis B. Ultrasound Med Biol. 2016;42:1026.
6. Srinivasa Babu A, Wells ML, Teytelboym OM, et al. Elastography in chronic liver disease: modalities, techniques, limitations, and future directions. Radiographics. 2016;36:1987–2006.
7. Jiao Y, Dong F, Wang H, et al. Shear wave elastography imaging for detecting malignant lesions of the liver: a systematic review and pooled meta-analysis. Med Ultrason. 2017;19:16–22.
8. Hashemi SA, Alavian SM, Gholami-Fesharaki M. Assessment of transient elastography (FibroScan) for diagnosis of fibrosis in non-alcoholic fatty liver disease: a systematic review and meta-analysis. Caspian J Intern Med. 2016;7:242–52.
9. Karagoz E, Ozturker C, Sonmez G. Noninvasive evaluation of liver fibrosis: supersonic shear imaging or acoustic radiation force impulse imaging? Radiology. 2016;279:979–80.
10. Peng Y, Qi X, Guo X. Child–Pugh versus MELD score for the assessment of prognosis in liver cirrhosis: a systematic review and meta-analysis of observational studies. Medicine (Baltimore). 2016;95:e2877.
11. Shetty K, Rybicki L, Carey WD. The Child–Pugh classification as a prognostic indicator for survival in primary sclerosing cholangitis. Hepatology. 1997;25:1049–53.
12. Lautt WW, Greenway CV. Hepatic venous compliance and role of liver as a blood reservoir. Am J Physiol. 1976;231:292–5.
13. Lee DH, Lee JM, Klotz E, et al. Multiphasic dynamic computed tomography evaluation of liver tissue perfusion characteristics using the dual maximum slope model in patients with cirrhosis and hepatocellular carcinoma: a feasibility study. Investig Radiol. 2016;51:430–4.
14. Klotz E, Haberland U, Glatting G, et al. Technical prerequisites and imaging protocols for CT perfusion imaging in oncology. Eur J Radiol. 2015;84:2359–67.
15. Feng YH, Hu XD, Zhai L, et al. Shear wave elastography results correlate with liver fibrosis histology and liver function reserve. World J Gastroenterol. 2016;22:4338–44.
16. Takahashi H, Ono N, Eguchi Y, et al. Evaluation of acoustic radiation force impulse elastography for fibrosis staging of chronic liver disease: a pilot study. Liver Int. 2010;30:538–45.
17. Hu X, Qiu L, Liu D, et al. Acoustic Radiation Force Impulse (ARFI) Elastography for non-invasive evaluation of hepatic fibrosis in chronic hepatitis B and C patients: a systematic review and meta-analysis. Med Ultrason. 2017;19:23–31.
18. Chen ML, Zeng QY, Huo JW, et al. Assessment of the hepatic microvascular changes in liver cirrhosis by perfusion computed tomography. World J Gastroenterol. 2009;15:3532–7.
19. Wang L, Fan J, Ding X, et al. Assessment of liver fibrosis in the early stages with perfusion CT. Int J Clin Exp Med. 2015;8:15276–82.
20. Guan S, Zhao WD, Zhou KR, et al. CT perfusion at early stage of hepatic diffuse disease. World J Gastroenterol. 2005;11:3465–7.
21. Kaufmann S, Horger T, Oelker A, et al. Characterization of hepatocellular carcinoma (HCC) lesions using a novel CT-based volume perfusion (VPCT) technique. Eur J Radiol. 2015;84:1029–35.
22. Rathmann N, Kara K, Budjan J, et al. Parenchymal liver blood volume and dynamic volume perfusion CT measurements of hepatocellular carcinoma in patients undergoing transarterial chemoembolization. Anticancer Res. 2017;37:5681–5.
23. Ippolito D, Sironi S, Pozzi M, et al. Perfusion computed tomographic assessment of early hepatocellular carcinoma in cirrhotic liver disease: initial observations. J Comput Assist Tomogr. 2008;32:855–8.
24. Hur S, Jae HJ, Jang Y, et al. Quantitative assessment of foot blood flow by using dynamic volume perfusion CT technique: a feasibility study. Radiology. 2016;279:195–206.
25. Zhan Y, Wu Y, Chen J, et al. Value of liver perfusion imaging of 256-slice CT in evaluation of the cirrhosis. Zhong Nan Da Xue Xue Bao Yi Xue Ban. 2016;41:44–50.
26. Motosugi U, Ichikawa T, Sou H, et al. Multi-organ perfusion CT in the abdomen using a 320-detector row CT scanner: preliminary results of perfusion changes in the liver, spleen, and pancreas of cirrhotic patients. Eur J Radiol. 2012;81:2533–7.

27. Van Beers BE, Leconte I, Materne R, et al. Hepatic perfusion parameters in chronic liver disease: dynamic CT measurements correlated with disease severity. AJR Am J Roentgenol. 2001;176:667–73.
28. Liu H, Liu J, Zhang Y, et al. Contrast-enhanced ultrasound and computerized tomography perfusion imaging of a liver fibrosis-early cirrhosis in dogs. J Gastroenterol Hepatol. 2016;31:1604–10.
29. Chang S, Kim MJ, Kim J, et al. Variability of shear wave velocity using different frequencies in acoustic radiation force impulse (ARFI) elastography: a phantom and normal liver study. Ultraschall Med. 2013;34:260–5.